

RESEARCH ARTICLE | NOVEMBER 18 2008

## Ferromagnetic Cu doped ZnO as an electron injector in heterojunction light emitting diodes

T. S. Herng; S. P. Lau; S. F. Yu; S. H. Tsang; K. S. Teng; J. S. Chen



*J. Appl. Phys.* 104, 103104 (2008)

<https://doi.org/10.1063/1.3021142>



Journal of Applied Physics

## Special Topics Open for Submissions

[Learn More](#)

# Ferromagnetic Cu doped ZnO as an electron injector in heterojunction light emitting diodes

T. S. Herng,<sup>1</sup> S. P. Lau,<sup>1,a)</sup> S. F. Yu,<sup>1</sup> S. H. Tsang,<sup>1</sup> K. S. Teng,<sup>2</sup> and J. S. Chen<sup>3</sup>

<sup>1</sup>*School of Electrical and Electronic Engineering, Nanyang Technological University, Nanyang Avenue, Singapore 639798, Singapore*

<sup>2</sup>*Multidisciplinary Nanotechnology Centre, School of Engineering, University of Wales Swansea, Singleton Park, Swansea SA2 8PP, United Kingdom*

<sup>3</sup>*Department of Materials Science and Engineering, National University of Singapore, Singapore 119260, Singapore*

(Received 29 July 2008; accepted 2 October 2008; published online 18 November 2008)

Ferromagnetic and highly conductive copper doped ZnO (ZnO:Cu) films were prepared by filtered cathodic vacuum arc technique. By employing a biasing technique during growth, the electron concentration and resistivity of the ZnO:Cu films can be as high as  $10^{20} \text{ cm}^{-3}$  and  $5.2 \times 10^{-3} \Omega \text{ cm}$ , respectively. The ferromagnetic behavior is observed in all the conductive films, but its magnetization is quenched with an increment in carrier concentration, suggesting that carrier induced exchange is not directly responsible for the ferromagnetism. Heterojunction light emitting diodes have been fabricated using the conductive ZnO:Cu layer as an electron injector and a *p*-type GaN as hole injector. Electroluminescence can be detected from the devices. © 2008 American Institute of Physics. [DOI: 10.1063/1.3021142]

## I. INTRODUCTION

The emerging field of spintronics has attracted significant attention since it promises new semiconductor device functionality through utilization of both electron charge and spin degree of freedom. It is desirable to achieve both semiconducting and magnetic properties within a single material system by doping nonmagnetic semiconductor with a small fraction of magnetic transition metal ions producing diluted magnetic semiconductors. The quest for copper doped ZnO (ZnO:Cu)<sup>1,2</sup> with Curie temperature ( $T_c$ ) above room temperature (RT) has gained momentum, following theoretical studies<sup>3,4</sup> that ZnO:Cu could be a promising candidate displaying RT ferromagnetism (FM). The fact that Cu and its oxides (CuO and Cu<sub>2</sub>O) are nonferromagnetic<sup>5</sup> removes any possibility of FM arising from the presence of secondary magnetic phases in this system. Our group<sup>6,7</sup> and Buchholz *et al.*<sup>8</sup> demonstrated RT FM in ZnO:Cu films. However, the realization of ZnO:Cu as a functional material for spintronics application has been a challenge. The performance of many RT ferromagnetic ZnO:Cu has been insufficient for use as functional material owing to their poor electrical properties.<sup>9,10</sup> The carrier concentration and conductivity reduce significantly with the incorporation of Cu. One of the possible ways to improve the conductivity of the ZnO-based sample is the utilization of substrate biasing technique during the film deposition. In this paper, we probe into the fabrication of highly conductive and yet ferromagnetic ZnO:Cu films by utilizing filtered cathodic vacuum arc (FCVA) in conjunction with substrate biasing technique at RT. The electron concentration of the ZnO:Cu films can be increased from  $10^{16}$  to  $10^{20} \text{ cm}^{-3}$ .

The realization of magnetic and conductive ZnO:Cu films is an essential step toward the fabrication of spin light emitting diodes (LEDs). Reproducible and stable *p*-type ZnO material with sufficiently high conductivity and carrier concentration is still in a development phase. Therefore, the fabrication of ZnO homojunction LEDs continues to be problematic.<sup>11,12</sup> In an alternative approach, the electron injection behavior of ZnO:Cu might be best exploited by constructing ZnO:Cu/GaN:Mg heterojunction LEDs. The *p*-type GaN:Mg can be served as hole injection layer and they have the same crystal structure (wurtzite) as ZnO with a small in-plane lattice mismatch ( $\sim 1.8\%$ ) and the same stacking sequence.<sup>13</sup> In the latter part of this paper, we report the fabrication and characterization of ZnO:Cu/GaN:Mg heterojunction LEDs. The appearance of electroluminescence (EL) signal gives an important insight that the ferromagnetic ZnO:Cu could be acted as an electron injector for LEDs.

## II. EXPERIMENTAL DETAILS

A series of ZnO:Cu films on Si substrates was prepared at RT by the FCVA technique. Zn:Cu alloy target containing 1 at. % of Cu was used in this experiment. The apparatus of FCVA has been described elsewhere.<sup>14</sup> During the deposition, O<sub>2</sub> was kept at 60 SCCM (SCCM denotes cubic centimeter per minute at STP) with a dc arc current of 60 A. To investigate the biasing effect, the substrate and sample holder were biased under various applied voltages, ranging from  $-200$  to  $+200 \text{ V}$  by a dc power supply during the film deposition. The magnetic properties of the ZnO:Cu films were investigated by an alternating gradient magnetometer with a maximum field of 10 kOe. To eliminate the spurious magnetic data, the ZnO:Cu samples and polymer tweezers were cleaned with acetone prior to magnetic measurement. The applied magnetic field was parallel to the surface of the

<sup>a)</sup>Author to whom correspondence should be addressed. Electronic mail: apsplau@polyu.edu.hk. Present address: Department of Applied Physics, Hong Kong Polytechnic University, Hung Hom, Hong Kong.

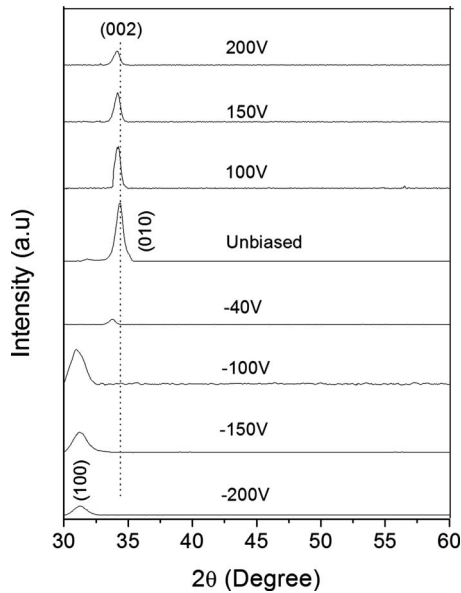


FIG. 1. XRD patterns of ZnO:Cu films deposited at various biasing conditions.

sample. The structural properties of the ZnO:Cu films were studied by x-ray diffraction (XRD). The conductive ZnO:Cu films on Si have made electrical analysis unfavorable, thus ZnO:Cu films were prepared on quartz substrates under identical conditions with ZnO:Cu on Si in order to study the electrical properties using van der Pauw method at RT.

### III. RESULTS AND DISCUSSION

The XRD patterns of the ZnO:Cu films are illustrated in Fig. 1. The XRD peaks of (100), (002), and (110) are perfectly indexed and they are corresponding to ZnO wurtzite structure. No secondary phases were detected within the sensitivity of XRD. It can be seen that the film deposited at RT without bias exhibited predominately *c*-axis (002) orientation. However, the intensity and full width at half maximum of (002) peak degrade with an increase in positive biased voltage. For the negative bias  $< -40$  V, the (002) peak disappears and the films change its predominated orientation to (100) direction with poor crystallinity as indicated by the broad and weak diffraction peak. A positive (negative) biased voltage is thought to attract negatively (positively) charged ions; the bombardment by these charged ions could deform the *c*-axis orientation and create an imperfect structure with large density of defects (i.e., Zn interstitial,  $Zn_i$  and/or O vacancies).<sup>15,16</sup> It is noted from Fig. 1 that negative biased samples showed poorer structural properties as compared to its positive biased counterparts. The heavier mass of positively charged particles (i.e., Cu and Zn) could generate higher impingement force to the negative biased samples, leading to dramatic deformation of structural properties. These results are consistent with Suzuki *et al.*<sup>16</sup> and Xu *et al.*<sup>17</sup> that the crystal orientation of ZnO is dependent on biased voltage and the negative biased samples generally exhibited poorer crystallinity as compared to positive biased samples. The (002) peak is shifted to a lower angle with an increase in biasing voltage, which indicates that the samples

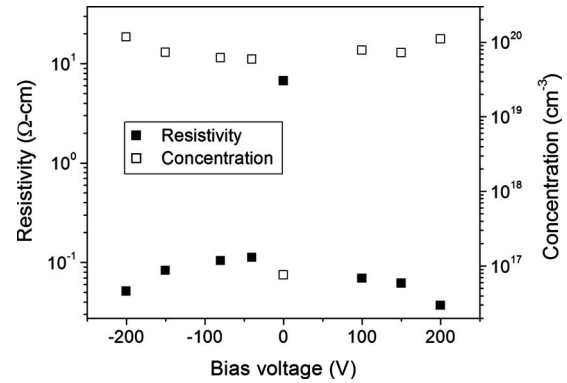


FIG. 2. Electrical resistivity and electron concentration of the ZnO:Cu films as a function of bias voltage.

exhibited larger lattice parameter *c*. Defects and imperfection in the grain of the biased ZnO:Cu lead to higher compression stress exerted on lattice resulting in a larger *c*.<sup>14</sup>

As illustrated in our previous work,<sup>9</sup> the incorporation of Cu into ZnO reduces its conductivity as Cu introduces deep acceptor level and it traps electrons from the conduction band.<sup>9,11</sup> However, with the biasing technique, all the prepared ZnO:Cu films are conductive with *n*-type behavior and its electrical properties are depicted in Fig. 2. The resistivity and carrier concentration of the unbiased ZnO:Cu film are  $6.7 \Omega \text{ cm}$  and  $7.6 \times 10^{16} \text{ cm}^{-3}$ , respectively. The carrier concentration of the biased ZnO:Cu increases drastically by four orders of magnitude to  $\sim 1.2 \times 10^{20} \text{ cm}^{-3}$ , whereas the resistivity reduces to  $\sim 3.7 \times 10^{-2} \Omega \text{ cm}$ . As the biased voltage increases, a flux of energetic atoms impinging on the substrate with increasing kinetic energy would cause a deviation from crystallinity, accompanied by a change in electrical properties. The structural defective ZnO:Cu led us to envisage that the enhanced electrical properties are related to the presence of structural defects (i.e.,  $Zn_i$  or/and O vacancies) in the films. The improved electrical properties in the ZnO:Cu films by the biasing technique are a common characteristic of doped ZnO film.<sup>15,18</sup>

Figure 3 shows the magnetic properties of the biased ZnO:Cu films. A well defined hysteresis loop was observed for the +100 V biased ZnO:Cu film with  $M_s$  of  $0.32 \mu_B/\text{Cu}$  and  $H_c$  of 98.5 Oe as shown in the inset of Fig. 3, showing a RT FM. The  $M_s$  of the ZnO:Cu samples prepared at various biasing conditions are normalized by the corresponding unbiased sample, where  $M_n = M_s(V)/M_s(\text{unbiased})$ . It is worthwhile to mention that the unbiased ZnO:Cu prepared at RT possessed the  $M_s(\text{unbiased})$  of  $0.4 \mu_B/\text{Cu}$ .<sup>19</sup> As depicted in Fig. 3, the  $M_s$  reduces with an increase in biased voltage. All the biased films possess weaker magnetic moment as compared to the unbiased ZnO:Cu film,  $M_n$  is  $< 1$ . These results elucidate that magnetic ordering depends on the applied bias; the transformation of the crystal orientation and quality would lead to the transition of FM to paramagnetism. Theoretical modeling of the ZnO:Cu system indicates that the location of the Cu atoms relative to each other and its substituted sites in host lattice can strongly affect the magnetic properties of the system.<sup>20-22</sup> Feng<sup>22</sup> studied the effect of Cu separation and the stability of the ferromagnetic state in

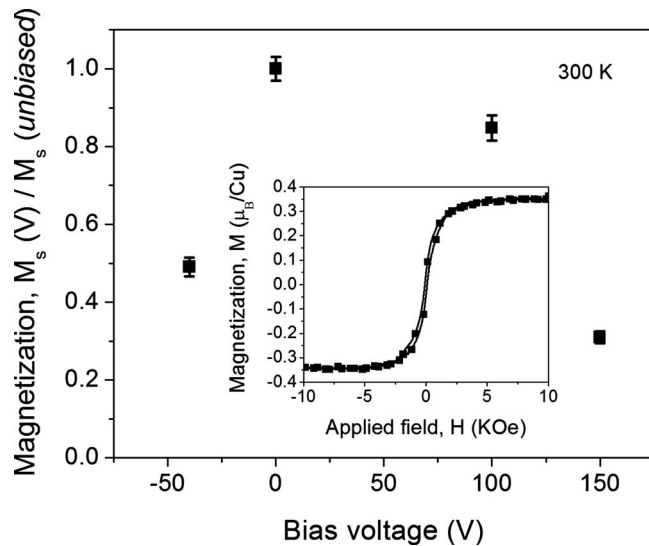


FIG. 3. Normalized saturated magnetic moment  $M_s$  of the ZnO:Cu films as a function of biasing voltage. Inset: magnetization curve of the ZnO:Cu prepared at +100 V.

ZnO:Cu. The FM is only possible to occur if two  $\text{Cu}^{2+}$  substitute two  $\text{Zn}^{2+}$  sites in  $c$ -plane, which gives a well separation distance at the lowest total energy at RT. However, if two  $\text{Cu}^{2+}$  ions are separated within the  $ab$  plane the antiferromagnetic state is favored, as evidenced by the absence of FM in the predominated (100) films. Taking the XRD and magnetic data together, it is noted that the magnetic moment reduces with increasing structural disorder. The presence of structural defects could suppress the magnetic ordering, which is in good agreement with recent literature.<sup>23,24</sup>

In addition to the Cu atom placement, the  $\text{Zn}_i$  also plays a significant role in enhancing and mediating magnetic ordering in the ZnO:Cu.<sup>19</sup> To investigate the role of  $\text{Zn}_i$  in the biased sample, the +100 V biased ZnO:Cu films were annealed at 200 and 400 °C under oxygen rich ambient for 1 h. The magnetic moment has been reduced by ~30% ( $0.22 \mu_B/\text{Cu}$ ) and ~45% ( $0.18 \mu_B/\text{Cu}$ ) for the samples annealed at 200 and 400 °C, respectively. It is attributed to the outdiffusion of  $\text{Zn}_i$  to the second nearest neighbor position as  $\text{Zn}_i$  has low diffusion barriers and easy to diffuse into the lattice at relatively low temperature.<sup>25</sup> As expected, the electrical properties of the films degrade with an increase in annealing temperature as shown in Fig. 4. After annealing treatment at 400 °C, the electron concentration of the biased

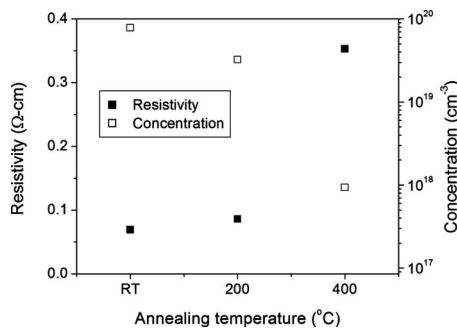


FIG. 4. Electrical resistivity and electron concentration of the +100 V biased ZnO:Cu film as a function of annealing temperature.

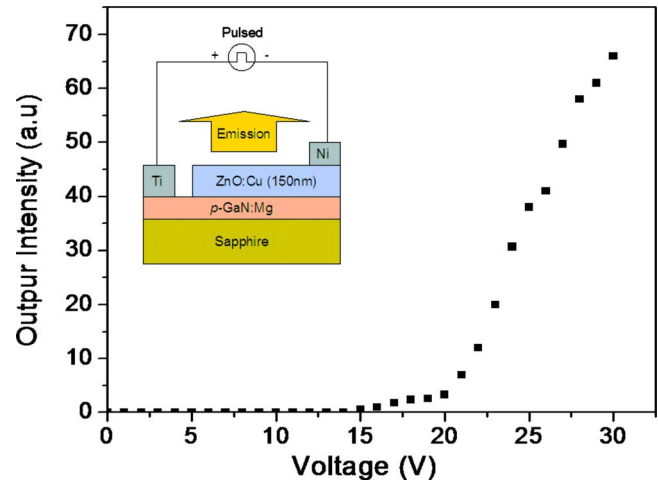


FIG. 5. (Color online) Current-voltage and light-voltage characteristics of the ZnO:Cu/p-GaN heterojunction LED. Inset: schematic illustration of the  $n$ -ZnO:Cu/p-GaN heterojunction LED structure.

ZnO:Cu reduced to  $9.33 \times 10^{17} \text{ cm}^{-3}$  with the resistivity of  $0.353 \Omega \text{ cm}$ . This result suggests that the deficiency of  $\text{Zn}_i$  in ZnO:Cu could degrade the magnetic ordering as well as electrical properties, which is consistent with the unbiased ZnO:Cu (control sample).

Now, let us explore the applicability of this ferromagnetic and conductive ZnO:Cu film as an electron injection layer in heterojunction LED. Among the samples, it is found that the ZnO:Cu prepared at the biased voltage of +100 V exhibited the highest  $M_s$ , considerably superior structural and electrical properties with carrier concentration of  $7 \times 10^{19} \text{ cm}^{-3}$ , thereby it was chosen for the heterojunction LED fabrication. The inset of Fig. 5 shows the schematic diagram of the proposed  $p$ - $n$  heterojunction diode (ZnO:Cu/p-GaN:Mg) with the size of  $6 \times 5 \text{ mm}^2$ . A 150 nm thick ZnO:Cu (1 at. %) was deposited on 1- $\mu\text{m}$ -thick  $p$ -GaN:Mg/sapphire (Technologies and Devices International, Inc.) with the hole concentration of  $\sim 1 \times 10^{18} \text{ cm}^{-3}$ . The contact layer of Ti (100 nm) and Ni (100 nm) was then e-beam evaporated onto the  $p$  and  $n$  layers, respectively.

The LED was biased under rectangle pulse voltage source (with repetition rate and pulse width of 12.6 and 60 ms, respectively) at RT and its corresponding light-voltage curve, which shows a rectifying behavior with a turn-on voltage of  $\sim 16 \text{ V}$ , is plotted in Fig. 5. The large turn-on voltage of the LED might be attributed to the interface defects between ZnO:Cu and GaN layer and the high Ohmic resistance from Ti/Ni contact on the  $p$ -GaN:Mg and ZnO:Cu. The interface defects and high contact resistance will lead to a high turn-on voltage of the LED.

Figure 6 shows the EL spectrum of the diode at different forward-biased voltages. The EL spectrum obtained in the sample is fitted by two Gaussian curves, which is dominated by broad blue and green luminescence bands peaking at 466 and 554 nm, respectively.<sup>12</sup> The peak intensity increases with an increase in biased voltage, indicating that the diode exhibits effective band radiative recombination. The appearance of EL signal provides important insight that the conductive  $n$ -ZnO:Cu is sufficient for electron injection in the heterojunction LED.



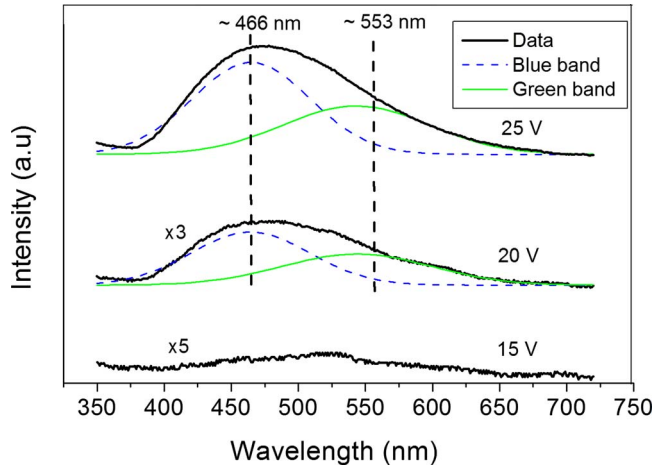


FIG. 6. (Color online) EL spectrum of the ZnO:Cu/p-GaN heterojunction LED at various forward bias.

The photoluminescence (PL) measurement was carried out on the ZnO:Cu film deposited on SiO<sub>2</sub>/Si substrate to examine the origin of EL emission and center of radiative recombination. The Nd:yttrium aluminum garnet laser source with a pump intensity of  $\sim 0.9$  MW/cm<sup>2</sup> was used in PL analysis. As expected, the PL spectrum consists of two components as depicted in Fig. 7. The peaks at 486 and 568 nm can be attributed to the blue and green luminescence bands, respectively. The PL spectrum is dominated by the green luminescence, whereas the blue luminescence dominates the EL spectra. The deviation in the PL and EL spectrum might be attributed to the influence of the heterointerface defect. Until now, the origin of this green emission is rather controversial.<sup>12</sup> Dingle<sup>26</sup> reported that the green luminescence was attributed to the introduction of Cu ions into ZnO, which has been supported by recent experimental observation by Alivov *et al.*<sup>27</sup> and Leiter *et al.*<sup>28</sup> In contrast, Studenikin and Cocivera<sup>29</sup> assigned the green luminescence to a donor-acceptor transition ( $D, A$ ) from oxygen vacancy ( $O_V$ ) to Zn vacancies ( $Zn_V$ ). On the other hand, Kang *et al.*<sup>30</sup> ascribed the appearance of the green luminescence to transitions involving deep levels within the band gap associated with oxygen vacancies. The annealing process that revealed

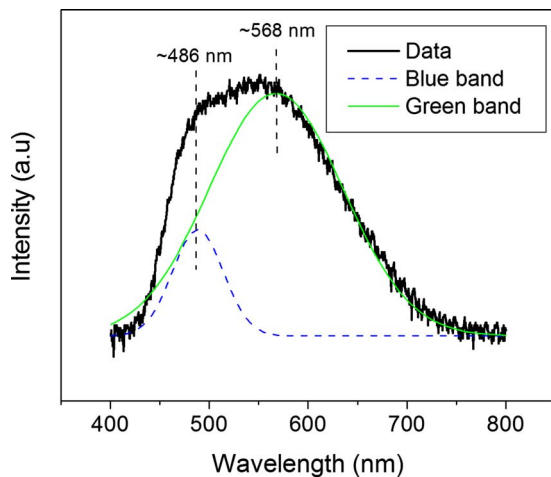


FIG. 7. (Color online) PL spectrum of the ZnO:Cu on SiO<sub>2</sub>/Si substrate.

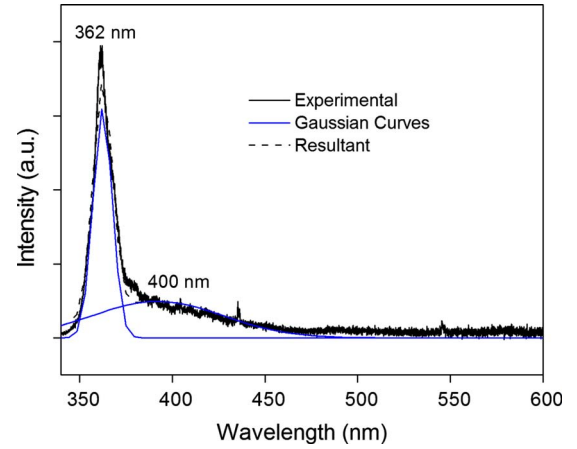


FIG. 8. (Color online) PL spectrum of the GaN:Mg film on sapphire substrate.

FM in our ZnO:Cu could be partially associated to the presence of  $Zn_i$ , thereby we proposed the broad green band would come from multiple energy levels in the forbidden band due to Cu or/and  $Zn_i$ . There is no ultraviolet (UV) peak observed in either PL or EL spectrum. The observation is consistent to the recent reports that the incorporation of Cu into ZnO could suppress the UV peak.<sup>27,31</sup>

To understand the origin of the blue emission band, the PL of the as-deposited GaN:Mg films was studied. Figure 8 shows the PL spectrum of the GaN:Mg film on a sapphire substrate. A sharp peak at  $\sim 362$  nm is observed with a tail extending to  $\sim 520$  nm. The curve can be fitted by two Gaussian curves at  $\sim 363$  and  $\sim 400$  nm. The emission at  $\sim 363$  nm is attributed to the near band edge emission of GaN:Mg, whereas the emission at  $\sim 400$  nm is likely to be the transition from the conduction band to the Mg acceptor level.<sup>32</sup> Hence, it is believed that the EL emission is not emerged from the GaN:Mg film. The proposed energy band diagram of  $n$ -ZnO:Cu/ $p$ -GaN:Mg is presented in Fig. 9. In this diagram, the electron affinity ( $\chi$ ) for ZnO:Cu and

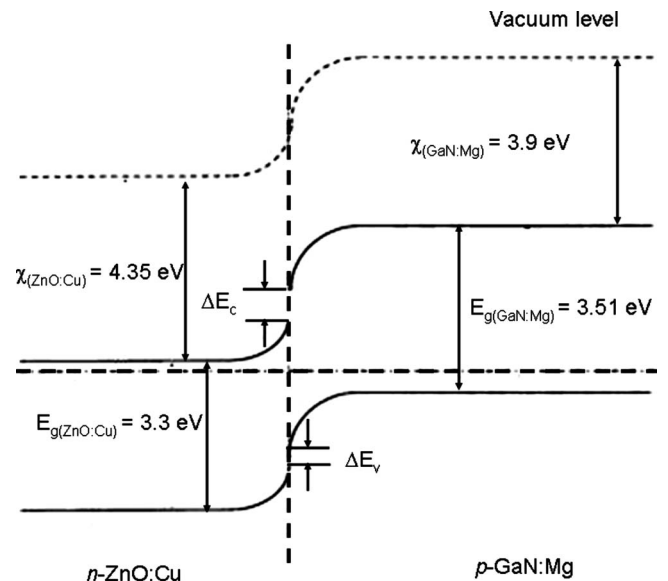


FIG. 9. Energy band diagram of the  $n$ -ZnO:Cu/ $p$ -GaN:Mg heterojunction.

GaN:Mg is taken as  $\sim 4.35$  and  $\sim 3.9$  eV, respectively. The bandgap ( $E_g$ ) for ZnO:Cu is assumed as  $\sim 3.3$  and  $\sim 3.51$  eV for GaN:Mg.<sup>33</sup> As can be seen from the diagram, the energetic barrier  $\Delta E_C$  for electrons is  $\Delta E_C = \chi_{(\text{ZnO:Cu})} - \chi_{(\text{GaN:Mg})} = (4.35 - 3.9)$  eV = 0.45 eV, while the energetic barrier  $\Delta E_V$  for holes is  $\Delta E_V = E_{g(\text{ZnO:Cu})} + \Delta E_C - E_{g(\text{GaN:Mg})} = (3.3 + 0.45 - 3.51)$  eV = 0.24 eV. Thus, the energetic barrier for holes  $\Delta E_V$  is  $\sim 2$  times less than the barrier for electrons  $\Delta E_C$ , showing a much smaller barrier for holes than that which exists for electrons. Thus, it is suggested that the EL emission emerges from the ZnO:Cu region of the device. In order to obtain band-to-band EL emission in the heterojunction LED, an intrinsic ZnO layer should be inserted between the ZnO:Cu and GaN:Mg layers. This work is currently underway and will be reported elsewhere.

It is recalled that the relatively high-resistive unbiased ZnO:Cu films exhibit higher magnetic moment as compared to the conductive films, although the latter possess a higher carrier concentration, thereby the FM in the conductive ZnO:Cu may not be carrier mediated.<sup>34</sup> The experimental results indicate that  $\text{Zn}_i$ , crystal quality, and crystal orientation play an important role in the magnetic moment of the conductive ZnO:Cu films. In this case, the highly nonequilibrium process of FCVA-biasing technique makes the  $\text{Zn}_i$  defects located throughout the lattice in the films; the interaction between  $\text{Zn}_i$  and  $\text{Cu}^{2+}$  ions in the lattice at the appropriate distance and density<sup>35</sup> will give rise to magnetic ordering in the ZnO:Cu according to the bound magnetic polarons (BMPs) model.<sup>36</sup> The annealing process has provided important insight into the role played by  $\text{Zn}_i$  in the ZnO:Cu system. It is worthy to highlight that the crystal orientation is crucial to the FM in the ZnO:Cu films in addition to  $\text{Zn}_i$ - $\text{Cu}^{2+}$  interaction, a (002) crystal orientation appears to be essential to the observation of magnetic ordering. However, it is not clear why conductive ZnO:Cu film will give a lower magnetic moment as compared to relatively high-resistive films, which is also a common characteristic for the conductive ZnO:Cu (Ref. 10) and ZnO:Co films.<sup>37,38</sup> Until now, the explanation of this phenomenon is rather controversial. Venkatesen *et al.*<sup>37</sup> reported that reduction in magnetization in the conductive ZnO:Co was attributed to the absence of cobalt nanoclusters, whereas Song *et al.*<sup>38</sup> suggested that the presence of the structure defects could enhance FM in insulating ZnO:Co films as compared to semiconducting films. Chakraborti *et al.*<sup>2,10</sup> proposed that carrier induced exchange was not directly responsible for the conductive ZnO:Cu samples but the BMP model. Here, we propose that the deviation in magnetic moment could be related to the defect density of the sample as certain critical defect density will lead to the optimized magnetic couplings.<sup>35</sup> Based on the BMP model, the magnetic properties of the ZnO:Cu films could be tuned through Cu and defects concentration, which are in good agreement with our results.

#### IV. CONCLUSION

In summary, conductive and ferromagnetic ZnO:Cu have been demonstrated using the biasing technique. The magnetization of the biased ZnO:Cu is correlated with its structural

properties, crystal orientation, and biasing voltage. The structural properties of the ZnO:Cu degrade with an increase in biasing voltage and lead to the transition of FM to paramagnetism. Furthermore, it is found that the crystal orientation [i.e., (002) oriented] and defect density are crucial to the FM in the ZnO:Cu. A  $n$ -ZnO:Cu/ $p$ -GaN:Mg heterojunction LED has been demonstrated. The heterojunction exhibited RT EL, showing the blue and green band luminescences. The appearance of EL signal is an important insight that the conductive ZnO:Cu can be acted as electron injector in LED. The realization of ZnO:Cu based LEDs may open up a new prospect for spin LEDs.

#### ACKNOWLEDGMENTS

One of the authors (S.P.L.) is grateful to The Royal Society of the United Kingdom for support through a travel grant. This project was partially supported by the Ministry of Education (Singapore) (Grant No. ARC 2/06).

- <sup>1</sup>D. J. Keavney, D. B. Buchholz, Q. Ma, and R. P. H. Chang, *Appl. Phys. Lett.* **91**, 012501 (2007).
- <sup>2</sup>D. Chakraborti, S. Ramachandran, G. Trichy, J. Narayan, and J. T. Prater, *J. Appl. Phys.* **101**, 053918 (2007).
- <sup>3</sup>L.-H. Ye, A. J. Freeman, and B. Delley, *Phys. Rev. B* **73**, 033203 (2006).
- <sup>4</sup>C.-H. Chien, S. H. Chiou, G. Y. Guo, and Y.-D. Yao, *J. Magn. Magn. Mater.* **282**, 275 (2004).
- <sup>5</sup>M. Wei, N. Braddon, D. Zhi, P. A. Midgley, S. K. Chen, M. G. Blamire, and J. L. MacManus-Driscoll, *Appl. Phys. Lett.* **86**, 072514 (2005).
- <sup>6</sup>T. S. Heng, S. P. Lau, S. F. Yu, H. Y. Yang, X. H. Ji, J. S. Chen, N. Yasui, and H. Inaba, *J. Appl. Phys.* **99**, 086101 (2006).
- <sup>7</sup>T. S. Heng, S. P. Lau, S. F. Yu, H. Y. Yang, L. Wang, M. Tanemura, and J. S. Chen, *Appl. Phys. Lett.* **90**, 032509 (2007).
- <sup>8</sup>D. B. Buchholz, R. P. H. Chang, J. H. Song, and J. B. Ketterson, *Appl. Phys. Lett.* **87**, 082504 (2005).
- <sup>9</sup>T. S. Heng, S. P. Lau, S. F. Yu, H. Y. Yang, K. S. Teng, and J. S. Chen, *J. Phys.: Condens. Matter* **19**, 236214 (2007).
- <sup>10</sup>D. Chakraborti, G. Trichy, J. Narayan, J. T. Prater, and D. Kumar, *J. Appl. Phys.* **102**, 113908 (2007).
- <sup>11</sup>S. J. Pearton, D. P. Norton, K. Ip, Y. W. Heo, and T. Steiner, *J. Vac. Sci. Technol. B* **22**, 932 (2004).
- <sup>12</sup>U. Ozgur, Y. I. Alivov, C. Liu, A. Teke, M. A. Reshchikov, S. Dogan, V. Avrutin, S.-J. Cho, and H. Morkoc, *J. Appl. Phys.* **98**, 041301 (2005).
- <sup>13</sup>P. Kung and M. Razeghi, *Opto-Electron. Rev.* **8**, 201 (2000).
- <sup>14</sup>Y. G. Wang, S. P. Lau, H. W. Lee, S. F. Yu, B. K. Tay, X. H. Zhang, K. Y. Tse, and H. H. Hng, *J. Appl. Phys.* **94**, 1597 (2003).
- <sup>15</sup>D. G. Lim, D. H. Kim, J. K. Kim, O. Kwon, K. J. Yang, K. I. Park, B. S. Kim, S. W. Lee, M. W. Park, and D. J. Kwak, *Superlattices Microstruct.* **39**, 107 (2006).
- <sup>16</sup>Y. Suzuki, M. Yoshitake, T. Yotsuya, K. Takiguchi, and S. Ogawa, *Nucl. Instrum. Methods Phys. Res. B* **37–38**, 854 (1989).
- <sup>17</sup>X. L. Xu, S. P. Lau, and B. K. Tay, *Thin Solid Films* **398–399**, 244 (2001).
- <sup>18</sup>H.-L. Ma, X.-T. Hao, J. Ma, Y.-G. Yang, S.-L. Huang, F. Chen, Q.-P. Wang, and D.-H. Zhang, *Surf. Coat. Technol.* **161**, 58 (2002).
- <sup>19</sup>T. S. Heng, S. P. Lau, S. F. Yu, J. S. Chen, and K. S. Teng, *J. Magn. Magn. Mater.* **315**, 107 (2007).
- <sup>20</sup>K. Sato and H. Katayama-Yoshida, *Jpn. J. Appl. Phys., Part 2* **39**, L555 (2000).
- <sup>21</sup>M. S. Park and B. I. Min, *Phys. Rev. B* **68**, 224436 (2003).
- <sup>22</sup>X. Feng, *J. Phys.: Condens. Matter* **16**, 4251 (2004).
- <sup>23</sup>W. B. Jian, Z. Y. Wu, R. T. Huang, F. R. Chen, J. J. Kai, C. Y. Wu, S. J. Chiang, M. D. Lan, and J. J. Lin, *Phys. Rev. B* **73**, 233308 (2006).
- <sup>24</sup>Z. Y. Wu, F. R. Chen, J. J. Kai, W. B. Jian, and J. J. Lin, *Nanotechnology* **17**, 5511 (2006).
- <sup>25</sup>A. F. Kohan, G. Ceder, D. Morgan, and C. G. van de Walle, *Phys. Rev. B* **61**, 15019 (2000).
- <sup>26</sup>R. Dingle, *Phys. Rev. Lett.* **23**, 579 (1969).
- <sup>27</sup>Y. I. Alivov, M. V. Chukichev, and V. A. Nikitenko, *Semiconductors* **38**, 31 (2004).

- <sup>28</sup>F. Leiter, H. Zhou, F. Henecker, A. Hofstaetter, D. M. Hofmann, and B. K. Meyer, *Physica B* **308–310**, 908 (2001).
- <sup>29</sup>S. A. Studenikin and M. Cocivera, *J. Appl. Phys.* **91**, 5060 (2002).
- <sup>30</sup>H. S. Kang, J. S. Kang, J. W. Kim, and S. Y. Lee, *J. Appl. Phys.* **95**, 1246 (2004).
- <sup>31</sup>Y. Yang, J. X. Wang, X. W. Sun, B. K. Tay, Z. X. Shen, and Y. Z. Zhou, *Nanotechnology* **18**, 6 (2007).
- <sup>32</sup>G.-C. Y. W. I. Park, *Adv. Mater. (Weinheim, Ger.)* **16**, 87 (2004).
- <sup>33</sup>U. Kaufmann, M. Kunzer, H. Obloh, M. Maier, C. Manz, A. Ramakrishnan, and B. Santic, *Phys. Rev. B* **59**, 5561 (1999).
- <sup>34</sup>J. Philip, A. Punnoose, B. I. Kim, K. M. Reddy, S. Layne, J. O. Holmes, B. Satpati, P. R. Leclair, T. S. Santos, and J. S. Moodera, *Nature Mater.* **5**, 298 (2006).
- <sup>35</sup>G. Bouzerar and T. Ziman, *Phys. Rev. Lett.* **96**, 207602 (2006).
- <sup>36</sup>J. M. D. Coey, M. Venkatesan, and C. B. Fitzgerald, *Nature Mater.* **4**, 173 (2005).
- <sup>37</sup>M. Venkatesan, P. Stamenov, L. S. Dorneles, R. D. Gunning, B. Bernoux, and J. M. D. Coey, *Appl. Phys. Lett.* **90**, 242508 (2007).
- <sup>38</sup>C. Song, X. J. Liu, K. W. Geng, F. Zeng, F. Pan, B. He, and S. Q. Wei, *J. Appl. Phys.* **101**, 103903 (2007).